JPPIPA 8(4) (2022)

Jurnal Penelitian Pendidikan IPA

Journal of Research in Science Education

http://jppipa.unram.ac.id/index.php/jppipa/index

Determination and Mapping of the Causes of High Risk of Earthquake Hazards Using Geoelectrical Data in Bengkaung, Batu Layar, West Lombok Indonesia

Hiden[1*], Suhayat Minardi[1], Syamsuddin Yasin[1], Bakti Sukrisna[1], Teguh Ardianto[1]

[1]Department of Physics, Faculty of Mathematics and Natural Sciences, University of Mataram, Indonesia.

Received: September 20, 2022
Revised: October 25, 2022
Accepted: October 29, 2022
Published: October 31, 2022

Corresponding Author:
Hiden
hidenpamula@unram.ac.id

DOI: 10.29303/jppipa.v8i4.2206

Abstract: The Bengkaung area, Batulayar District, West Lombok is suspected to be very vulnerable to the risk of earthquake hazards. However, in this area no scientific research, either geological or geophysical, has ever been carried out regarding this hazard. How are the physical characteristics of the lithology and structure in the area to the risk of earthquake disaster? The purpose of this study was to determine the physical characteristics of the lithology and subsurface structures that were validated by the level of damage. The method used is the geoelectric method and local building damage data. The results of the 2D geoelectric anomaly modeling show the characteristics of the subsurface lithological layers in the form of sand, sandstone, clay, andesite lava faults, fresh andesite lava, and granite. The fault was detected in the center of the study area in a north-south direction. Earthquake hazard analysis shows that the cause of the high risk of earthquake hazard in Bengkaung Village is the presence of faults and cohesive lithology. The highest potential risk is in the southern part of Bengkaung Village. The southern area of Bengkaung Village is dominated by clay that has cohesive properties, especially on the surface. The western and northern parts of Bengkaung Village have medium and low vulnerability to earthquake hazards. The last two areas are dominated by non-cohesive soils in the form of sandy soils and lapilli pumice.

Keywords: Bengkaung; Earthquake; Geoelectrical; Vulnerability

Introduction

Natural disasters are disasters caused by nature in the form of earthquakes, tsunamis, volcanic eruptions, floods, droughts, hurricanes, and landslides (Law No. 24 of 2007 concerning Disaster Management). One of the natural disasters that often occur in Indonesia is an earthquake. Earthquakes are disasters that can take lives and cause damage to buildings (BNPB, 2007).

The history of earthquakes in Lombok records several large earthquakes that have occurred, at least 10 times before 2018. The first recorded earthquake was July 25, 1856 in Labuan Tereng with a magnitude of 6.0 on the Richter Scale (SR) that hit Ampenan Beach. Mataram and triggered a tsunami. Second, another earthquake with a magnitude of 6.0 on the Richter Scale occurred in South Lombok on December 21 and 24, 1970, and on May 28, 1972 another earthquake occurred in the south of Praya City at a distance of 262 km with a magnitude of 6.7 on the Richter Scale and caused several buildings to collapse. heavily damaged (USGS, 2021).

2018 was the year with the longest earthquake duration in the world (more than one month) with a strong magnitude. The first strong earthquake measuring 6.4 on the Richter Scale occurred at 06.47 (WITA: local time) on July 29 2018, with an epicenter 47 km northeast of Mataram City. The shaking of this earthquake was felt in all areas of Lombok Island, Bali Island and Sumbawa Island. This earthquake was the first in a series of at least 585 earthquake events as of August 5, 2018 at the same location as the first incident, with the largest strength in the history of the Lombok

How to Cite:
Hiden, H., Minardi, S., Yasin, S., Sukrisna, B., & Ardianto, T. (2022). Determination and Mapping of the Causes of High Risk of Earthquake Hazards Using Geoelectrical Data in Bengkaung, Batu Layar, West Lombok Indonesia. *Jurnal Penelitian Pendidikan IPA*, *8*(4), 2404–2410. https://doi.org/10.29303/jppipa.v8i4.2206

earthquake, which was 7.0 on the Richter Scale. This second earthquake caused severe damage in Lombok: North, East and West (USGS, 2021). Furthermore, the third major earthquake occurred on August 19, 2018 at 20:56 WITA with a strength of 7.0 on the Richter Scale. This third major Lombok earthquake occurred in Sambelia, East Lombok at a hypocenter depth of 25 km. This earthquake resulted in 460 fatalities and 71,962 houses were seriously damaged (BMKG, 2018).

One of the worst impacts of this third earthquake was in Bengkaung Village, Batu Layar District, West Lombok. Based on data (BPBBD, 2021) this third strong earthquake resulted in 328 houses being heavily damaged, 207 houses being moderately damaged, and 271 houses being lightly damaged. We also found direct damage remnants at the site as shown in Figure 1 (Lavigne et al., 2020). The pattern of damage phenomena in Bengkaung Village approaches a straight line in a north-south direction. We suspect that the phenomenon of damage such as this line is an indication of faults and soft soil that is vulnerable to earthquake hazards.

Disaster-prone areas other than sandy soils, soils that are more susceptible to liquefaction are mixed soil deposits such as silty sand, silt, silty clay, clay, or other combinatorial soils. Severe damage occurred to the soil structure such as large soil deformation and the collapse of the embankment due to the collapse of the base layer (clay) during an earthquake (Hyodo et al., 1993).

Based on the description of the background above, it is very important to take steps to mitigate the earthquake disaster, in order to reduce the risk if an earthquake occurs again, especially in Bengkaung Village, Batu Layar. One of the earthquake disaster mitigations that can be done is to know the causes and map the locations that are prone to earthquake hazards. Therefore, it is very important to know the physical characteristics of the lithology and subsurface structures as well as soft soils that are susceptible to earthquake or liquefaction hazards at the study site. The purpose of this study was to map earthquake-prone areas in Bengkaung Village, Batu Layar based on the lithological characteristics and structure of the study area. These lithological and structural characteristics can be identified by mapping and 2D geoelectric resistivity modeling in the area.

Analysis of lithological physical characteristics based on structural models and soft soils that are susceptible to high earthquake hazard risks, in this paper focused on 2D Geoelectric data and compared with the results of the geomagnetic model (Amin et al., 2022). From the geoelectrical resistivity data, it can be seen the physical characteristics of the subsurface lithology, structural model, and soft soil (Kolawole et al., 2018; Rosyidi et al., 2008; Minardi et al., 2021). So that the dangers that may occur in Bengkaung Village can be reduced (mitigation). The results of this study also contribute to the field of geophysics and as a basis for making strategic policies for the government and related agencies.

Figure 1. Damage photos: a) and b) in Bangkaung Village, c) in Senggigi (Northwest of Bengkaung), d) in Sandik Village (South Bengkaung) (Hyodo et al., 1993)

Method

Geoelectrical Resistivity is a method that we use to study subsurface lithology based on the nature of the flow of electricity to rocks below the earth's surface. The working principle of this method is that an electric current is injected into the earth through two current electrodes, then the potential difference that occurs is measured through two potential electrodes. The measurement results in the form of current and potential differences for each different electrode distance (Figure 2) will provide different variations in resistivity values according to the lithological layer below the surface **(**Reynolds, 1997).

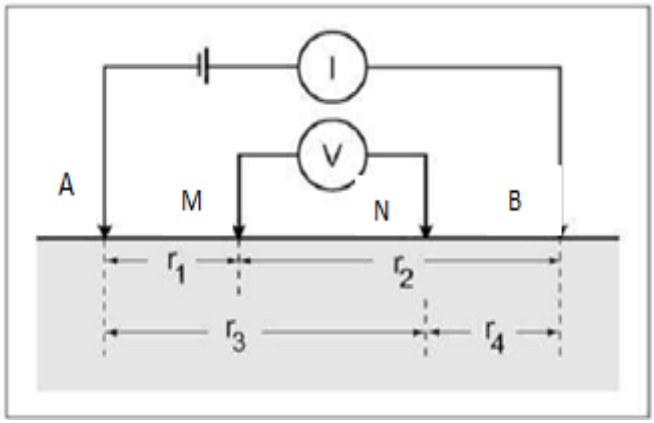

Figure 2. Wenner configuration (Reynolds, 1997)

In this Wenner configuration (Figure 2), the four electrodes are lined up at equal electrode intervals: and the current electrodes (A and B) are outside the potential electrodes (M and N). This arrangement is generally used for profiling to determine the resistivity contrast of rocks horizontally (mapping). Wenner configuration with the distance between the electrodes AM=MN=NB=a. The value of the measured potential difference between the M and N electrodes is expressed as:

$$\Delta V = \frac{\rho I}{2\pi}\left[\left(\frac{1}{r_1}-\frac{1}{r_2}\right)-\left(\frac{1}{r_3}-\frac{1}{r_4}\right)\right] \quad (1)$$

or form of resistivity,

$$\rho = 2\pi a \frac{\Delta V}{I} \quad (2)$$

Where $r_1 = r_2 = r_3 = r_4 = a$

In this study, 2D geoelectric data from field surveys were used, to determine the subsurface structure in detail, which was previously indicated by geomagnetic residual anomaly data (Amin et al., 2022). 2D geoelectrical measurements were carried out at locations where faults were suspected and which had high contrast geomagnetic anomalies (Figure 3). This high-contrast geomagnetic anomaly is thought to be caused by a fault and has been filled or covered with sediment. Geomagnetic anomalies are interpreted qualitatively and quantitatively (Reynolds, 1997). As with 2D geomagnetic structure modeling, geoelectrical data are also interpreted with advanced modeling methods and then reversed, to find out subsurface rock strata/structures in more detail.

Result and Discussion

Total Magnetic Field Anomaly

Figure 3 is an anomaly of the residual geomagnetic field with a range of values between minus 1200 nT to 1650 nT. High anomalies are shown in purple and low anomalies are shown in blue. High magnetic anomalies are related to magnetic objects that have high magnetic susceptibility values or fields, such as lava, and basalt. On the other hand, the low anomalous value is caused by objects that have low magnetic susceptibility values below the surface, such as clay, pumice, sand, and others in the study area.

2D Geoelectric Data

The geoelectric profile was obtained based on the residual magnetic anomaly contour map (Figure 3) to determine the details of the subsurface strata/structure in the study area. Figure 4a is a 2D inverted geoelectrical section obtained from the southern part of the study site. This profile has a longitudinal direction in an East-West direction around the DD' profile in Figure 3. At first glance, the two geomagnetic and geoelectrical cross-sectional images (Figures 3 and 4a) match mainly the height anomaly. We then interpret a 2D resistivity model of this inversion to determine the type of local subsurface lithology. The color scale shows the distribution of the actual resistivity values, which are then grouped by taking into account the color contrast as the boundary between groups. We grouped Figure 4a based on resistivity values into three layer groups. The layer groups are successively from the local soil surface, namely: red to brownish red with a resistivity value of 15.5 ohm-m to 38.8 ohm-m. The second layer has a resistivity value of 4.68 ohm-m to 15.5 ohm-m and the third layer is blue with a resistivity value of 0.96 ohm-m to 4.68 ohm-m.

The interpretation of each layer group is matched with direct observations in the field, reference tables, and geological formations in the study area. The first layer is 5 – 10 m thick at 0 – 160 m horizontally. This layer consists of clay containing pumice, pumice (lapilli), and a layer of pumice breccia sand. This layer corresponds to outcrops in the field. The overburden layer with a thickness of 0.5 m is a clay layer containing pumice covering a 1.6 m thick layer of falling pumice and a 1 m thick volcanic breccia layer exposed at the site. This pumice layer is pumice that fell from the eruption of Mount Samalas in 1257. Under the pumice layer there is a layer of breccia sand that covers the clay layer below (Paleo-topography). This layer of quicksand and breccia covers almost the entire island of Lombok (Hiden et al., 2014; Hiden et al., 2017).

The second layer, green to yellow with a resistivity value of 4.68 ohm-m to 13.5 ohm-m (Figure 4a) is interpreted as volcanic breccia. This volcanic breccia rock layer occupies a depth of 5 m to 30 m from the local surface at a position of 40 - 160 m horizontally. The third layer, colored blue with resistivity values of 0.88 ohm-m to 5.10 ohm-m, runs along the line and fills in depths ranging from 20 m. This layer is thought to be loose rock mixed with clay and sand. This is in accordance with the results of research (Putri et al, 2021), that soft soil (medium category) is weathered rock including loose rock mixed with clay and/or fine sand.

Figure 4b is a 2D reverse geoelectrical section obtained from line-2 in the center of the study site (line BB' in Figure 3) which extends east-southeast. The low resistivity value (shown between the two red arrows) is considered the boundary of the intrusion body (see Figure 3). Based on the color scale in Figure 4b, it can be seen that the resistivity values from the local soil surface are: red to brownish red with resistivity values from 16.4 ohm-m to 52.8 ohm-m. The second layer has a resistivity value between 5.10 ohm-m to 16.4 ohm-m and the third layer is blue with a value of 0.88 ohm-m to 5.10 ohm-m.

The results of the interpretation of each layer group consisting of clay containing pumice, lapilli pumice, and volcanic breccia sand according to outcrops in the field (Figure 5). The overburden layer fills the elevation of 25 – 40 m, successively the falling pumice layer is 1.6 m thick and the sandy pumice is 1 m thick and weathered breccia sand. The last two layers are alternating, indicating an iterative depositional process.

The second layer is green to yellow with a resistivity value of 5.10 ohm-m to 16.4 ohm-m (Figure 4b) is a volcanic breccia. The volcanic breccia layer along line-2 (BB') occupies an elevation of 20-25 m from the local surface. The third layer (Figure 4b), colored blue with resistivity values of 0.88 ohm-m to 5.10 ohm-m, runs along the line and occupies elevations from 20 m down. This layer is thought to be loose rock mixed with clay. This is in accordance with the results of research (Amin et al., 2022) that soft soil of medium category is weathered rock including loose rock mixed with clay and/or fine sand.

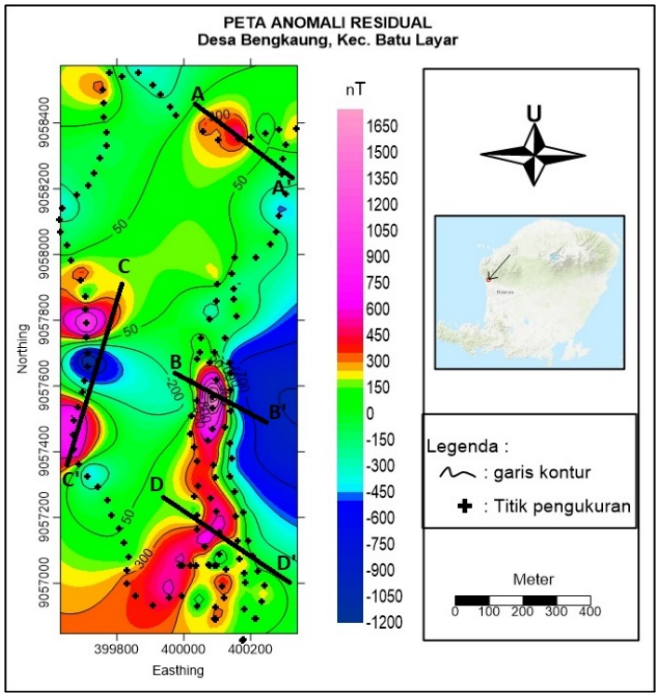

Figure 3. The Contour of residual anomaly (Amin et al., 2022)

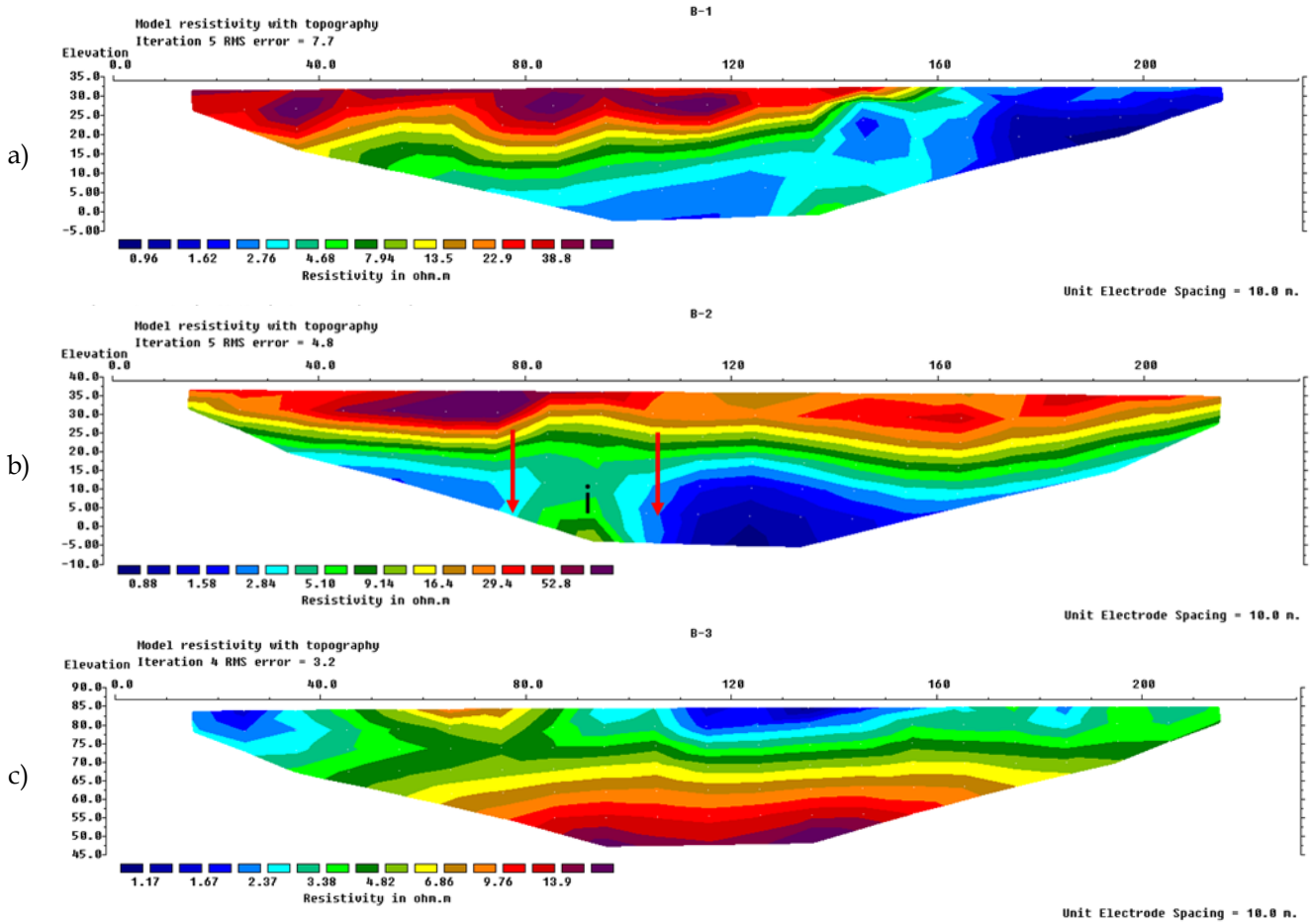

Figure 4. Cross-section of the resistivity structure of the study area: a) Line-1, b) Line-2, and c) Line-3

Figure 5. Outcrop of fallen pumice on line-2

The interesting thing on this line-2 (BB') is that there is a medium resistivity value of 5.10 ohm-m to 16.4 ohm-m (green to yellow color) subsurface, starting from an elevation of 25 m down and at a position of 80 – 115 m in the horizontal direction. Volcanic breccia material at this position appears to intrude on layers of loose rock mixed with clay to a height of about 25 m above sea level. This intrusive material is suspected to be the cause of the anomaly height shown in the -BB' line in Figure 3. This is in accordance with the 2D geomagnetic model in Figure 7 at a position of 77 – 177 m horizontally with a depth of more than 27 m (Amin et al., 2022). The second layer has a susceptibility value of SI which is a layer of clay resulting from weathering of breccia rocks. These rocks are at a depth of 27 m - 40 m. The third layer has a susceptibility value of in SI which is a fractured andesite lava rock, at a depth of 8 m - 63 m. in SI which is a fractured andesitic lava rock (Hiden et al., 2014), at a depth of 8 m - 63 m.

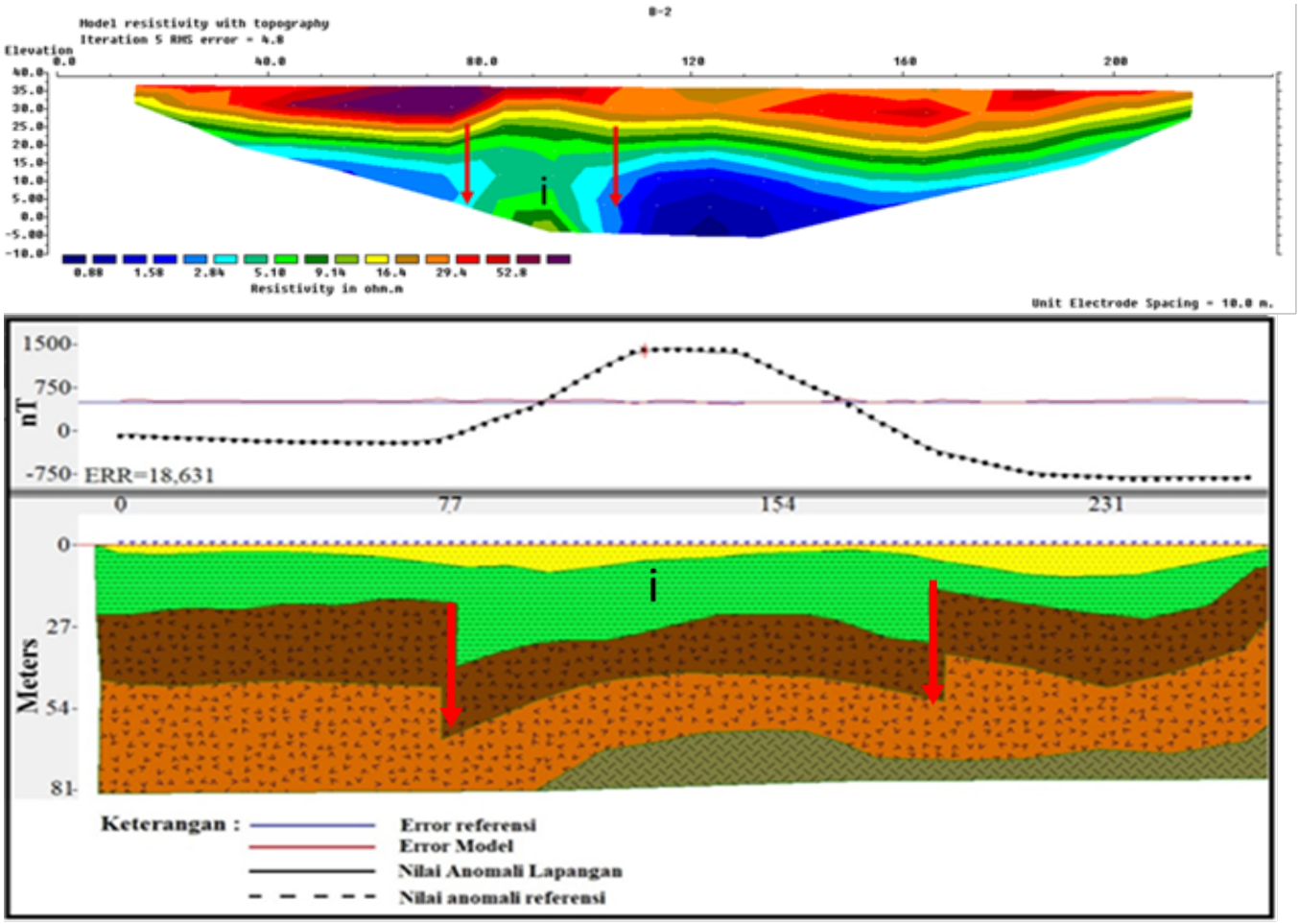

Figure 6. Structure of the 2D model of the BB geomagnetic anomaly trajectory

Figure 4c is an inverted 2D geoelectrical section obtained from line-3 in the northern part of Bengkaung Village around line AA' in Figure 3. Based on the color scale in Figure 4c, it can be seen the opposite of the previous two sections. In this 3-line cross section (AA'), low resistivity values occupy successive layers of the local soil surface, namely: blue with resistivity values of 1.17 ohm-m to 3.38 ohm-m. The second layer is green to yellow with resistivity values between 3.38 ohm-m to 6.86 ohm-m, and the third layer is yellow to brownish red with a value of 6.86 ohm-m to 13.9 ohm-m.

The results of the interpretation of each layer group consist of clay containing pumice, volcanic breccia sand layers containing clay, according to outcrops in the field (Figure 7). This topsoil fills at an elevation of 60 – 85 m, along the line, with resistivity values of 1.17 ohm-m to

3.38 ohm-m. The second layer of green to yellow color occupies an elevation of 60 – 85 m from the local surface along line-3. The resistivity value of this second layer is 3.38 ohm-m to 6.86 ohm-m which is thought to be volcanic breccia and altered lava. The third layer is a yellow to brown peacock with a resistivity value of 6.86 ohm-m to 13.90 ohm-m, starting from positions 55 – 185 m and occupying elevations ranging from elevations of 70 m and below. This layer is thought to be fresh lava rock and tuff breccia. The rock type in this third layer is thought to be a continuation of the intrusion on the two lines to the south.

Figure 7. Overburden outcrop on Line-3

Clay and silty clay are cohesive soils that are susceptible to liquefaction and are dynamic. The dynamic properties of cohesive soils are influenced by parameters: effective stress, shear strain, plasticity index, loading frequency, number of loading cycles, void ratio, degree of saturation, overconsolidation ratio, and particle size (Kumar et al., 2018). The dynamic properties of compressive cohesive soils are needed in most civil engineering constructions, such as the construction of dams, embankments, embankments, and others. Dynamic properties such as shear modulus, damping ratio, and Poisson soil ratio. The effect of confining stress and shear strain on the dynamic properties of cohesive soils causes an increase in the shear modulus and a decrease in the damping ratio and the Poisson ratio of the soil. The shear modulus of the soil decreases with increasing shear strain. This is due to the loss of soil stiffness with increasing shear strain. Dutta and Saride (2015) suggested that the variation of the soil shear modulus depends on the strain from a very small cohesive soil to a shear strain of 0.001% and thereafter decreases drastically.

Based on the interpretation of the lithological type from the resistivity values above, the soil surface is generally filled with clay to an average depth of 15 m. Clay layer is one type of cohesive lithology which has a high vulnerability to the risk of danger in the event of an earthquake. This is because when an earthquake occurs, the soil (clay) experiences very high pressure (depending on the strength of the earthquake and the location of the source) which results in a decrease in the shear modulus. This decrease in shear modulus is caused by the loss of soil stiffness with increasing shear strain. This is consistent with what we observed directly at a location where houses were generally heavily damaged (Figure 1).

Another cause of high vulnerability to earthquake hazards besides clay is the presence of faults (Figure 6) at the study site. Seismic events on the fault cause a decrease in cohesion due to the failure process. This decrease in cohesion contributes directly to the decrease in seismic stress. The associated increase in differential stress production in the reservoir leads to an increase in the number of more cohesive seismically activated faults (Ogo et al., 2018; Shapiro and Dinske, 2021). Thus, the presence of a fault in Bengakaung Village will increase vulnerability to disaster risk in the event of an earthquake. The provisional conclusion is that the southern to the central part of Bengkaung Village is vulnerable to earthquake hazards, while the northern and western parts are relatively safe.

Conclusion

Based on the results of the survey and analysis of Geoelectrical data verified by the level of damage to buildings on the site, it can be concluded that the main cause of high vulnerability to earthquake hazards in Bengkaung is the presence of cohesive soil and disturbances. Specifically, (1) The structure/strata of the subsurface layer from the south to the center of the study area consists of clay containing pumice, a layer of pumice (lapilli), and volcanic breccia sand. Layers of cracked andesite lava rock, fresh andesite lava, and granite rock layers; (2) The southern area of Bengkaung Village is dominated by cohesive soil in the form of clay with an average thickness of 15 m, making it prone to high earthquake risk. Meanwhile, the western and northern parts of Bengkaung Village are dominated by non-cohesive soils such as sand and pumice (lapilli) so that their vulnerability is relatively lower to the risk of earthquake hazards.

Acknowledgements

We thank the Head of Bengkaung Village, for allowing us to collect geomagnetic data in his area. Thank you to all those who have helped in this research, especially the discussion friends.

References

Amin, M., Hiden, H., & Minardi, S. (2022). Identification of Earthquake Hazard Vulnerability in Bengkaung Village, West Lombok Using Geomagnetic

Methods. *Jurnal Penelitian Pendidikan IPA*, *8*(2), 548–557. https://doi.org/10.29303/jppipa.v8i2.1338

BMKG. (2018). Jakarta City, 2018, diunduh pada link http://repogempa.bmkg.go.id/repo_new/repository.php

BNPB. (2007). Jakarta City, 2007, No. 66. https://bnpb.go.id//definisi-bencana

BPBD, Lombok Barat, Data kerusakan bangunan di Desa Bengkaung, 2021.

Dutta, T. T., & Saride, S. (2015, October). Dynamic properties of compacted cohesive soil based on resonant column studies. In *Int Conf Geo-Engg Climate Change Technologies for Sustainable Environ Manag, MNNIT Allahabad* (pp. 1-6).

Hiden, H., Brotopuspito, K. S., Sri Hadmoko, D., Lavigne, F., Airaksinen, K. B., Mutaqin, B. W., ... & Suryanto, W. (2017). The isopach mapping of volcanic deposits of Mount Samalas 1257 AD based on the values of resistivity and physical properties. *Geosciences*, *7*(3), 67.

Hiden, H., Kirbani, S. B., Hadmoko, D. S., & Setiawan, A. (2014). Accuracy and Automatic Computation of Seismic Refraction: a case of Forward Modeling and Inversion. *Gravitasi*, *13*(1).

Kumar, S.V., & Day, A.M.K.A. (2018). Dynamic properties and liquefaction behaviour of cohesive soil in northeast India under staged cyclic loading. *Journal of Rock Mechanics and Geotechnical Engineering*. 10(5). https://doi.org/10.1016/j.jrmge.2018.04.004

Lavigne, F., Jean, V., Suwardji, S., Kusnadi, K., Edong, E., Hiden, H., ... & Malawani, M. N. (2020, June). Earthquakes and tsunamis in Lombok, NTB: from hazard assessment to crisis management. In *Proceeding International Conference on Science (ICST)* (Vol. 1, No. 1, pp. 320-326).

Minardi, S., Mudyanto, A., & Hiden, H. (2021). Subsurface Structure Models of Sumbawa Island And Flores Back Arc Thrust Based On Gravity Data. *Jurnal Penelitian Pendidikan IPA*, *7*(3), 414-421.

Ogo, K., Hazarika, H., Kokusho, T., Matsumoto, D., Ishibashi, S., & Sumartini, W. O. (2018, March 9). Analysis of liquefaction of volcanic soil during the 2016 Kumamoto Earthquake based on boring data. *Lowland Technology International*, *19*(4, March), 245-250. Retrieved from https://cot.unhas.ac.id/journals/index.php/ialt_lti/article/view/524

Putri, S. R. E., Minardi, S., & Hiden, H. (2021). Penentuan Karakteristik Mekanisme Gempa Tahun 2018-2019 Di Nusa Tenggara Menggunakan Metode Inversi Momen Tensor. *Kappa Journal*, *5*(1), 31-39. https://doi.org/10.29408/kpj.v5i1.3315

Reynolds, J. M. (1997). *Geophysics*. Chichester John Wiley and Sons Ltd. 796p.

Shapiro, S.A., Dinske, C. (2021). Stress Drop, Seismogenic Index and Fault Cohesion of Fluid-Induced Earthquakes. *Rock Mech Rock Eng* **54**, 5483–5492. https://doi.org/10.1007/s00603-021-02420-3

USGS, (2021). *https://earthquake.usgs.gov*. Diakses pada bulan Februari 2021.